# Anion-driven mesogenicity: ionic liquid crystals based on the [*closo*-1-CB₉H₁₀]⁻ cluster†

Bryan Ringstrand,[*a*] Hirosato Monobe[*b*] and Piotr Kaszynski[*\*a*]

Two series of structurally analogous esters (**1**) and diazenes (**2**) derived from the [*closo*-1-CB₉H₁₀]⁻ anion and containing two or three rings in the rigid core were prepared and their liquid crystalline properties investigated. Salts containing NMe₄⁺ or NHEt₃⁺ counterion do not exhibit mesophases, whereas the ion pairs with *N*-butyl-4-heptyloxypyridinium cation **[Pyr]** exhibit SmA and occasionally soft crystalline phases in the temperature range of 90–180 °C. Three representative ionic liquid crystals, **1d[Pyr]**, **1f[Pyr]** and **2d[Pyr]**, were investigated by powder XRD. Absorption spectroscopy demonstrated that ester **1e[Pyr]** is transparent above 280 nm and the diazene **2e[Pyr]** exhibits absorption bands typical for azobenzene derivatives.
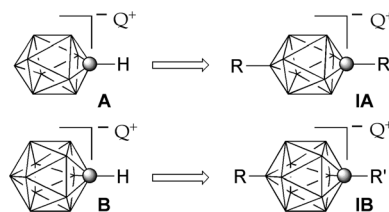
## Introduction

During the past decade, research of ionic liquid crystals (ILCs) has significantly intensified and diversified.[1] Among many intriguing properties, anisotropic ion mobility exhibited by some ILCs generated considerable interest in developing ion-conductive materials[2–6] for applications in batteries[7] and dye-sensitized solar cells.[8] It has been established that the nature of the counter anion plays a critical role in the properties.[9] For instance, high ion-conductivity is observed for salts in which the negative charge of the anion is delocalized and has weak electrostatic interactions with the accompanying mesogenicity-driving cation.[4] Another important aspect of ILCs is their photophysical behavior; judicious choice of the π chromophore allows to obtain photoresponsive,[10] highly luminescent,[11] or NLO active ionic mesogens.[12] In some pyridinium ILCs containing iodide[13,14] or bromide[15] as the counter anion, charge-transfer phenomena have been observed. This suggests potential applications for ILCs in photovoltaics, which is the driving force for the operation of solar energy conversion devices.[16]

The vast majority of ILCs investigated to date comprise of an organic cation, such as ammonium,[3,17] imidazolium,[4,6,18,19] or pyridinium,[13,20,21] that drives mesogenicity. In general, the anion in these materials is present for charge compensation, but it can significantly affect mesophase stability and the clearing temperature of the bulk material.[1] ILCs in which the anion drives the mesogenic behavior are rare, and in which the ions are in the fully dissociated state are difficult to design. Such materials, especially lithium salts, are sought after for their potential applications as

electrolytes for *e.g.* lithium ion batteries. The closest examples of such ILCs are alkali-metal carboxylates,[22] phosphates,[23] and phosphonates,[24] but their tight oxygen–metal interactions limit the ion conductivity in the neat phase and usefulness as an electrolyte. For this reason binary systems of non-ionic liquid crystal hosts, which contain groups capable of metal ion coordination (typically an oligoethylene oxide chain), and highly ionic metal salts are used to obtain anisotropic metal ion conductivity.[25]

*closo*-Monocarbaborates [*closo*-1-CB₉H₁₀]⁻ and [*closo*-1-CB₁₁H₁₂]⁻ (**A** and **B**, Fig. 1) are particularly attractive structural elements for ILCs due to their electronic and geometrical features.[26,27] In both structures, the negative charge is fully delocalized over the cage, and the clusters are among the least nucleophilic anions.[28] For this reason, clusters **A** and **B** and also some other *closo*-borates have been investigated as counterions in ionic liquids[29] and for applications as lithium-ion battery electrolytes.[30,31] The geometry of the two *closo* clusters **A** and **B** is appropriate for the formation of calamitic liquid crystals, as can be inferred from results for their electrically neutral carborane analogues.[32–39] As a consequence of the molecular symmetry, clearing temperatures for the 12-vertex carborane derivatives are generally higher than those for the 10-vertex analogues.[32,34,36,38] On the other hand, the symmetry of and the energy associated with molecular orbitals allow for much more efficient electronic
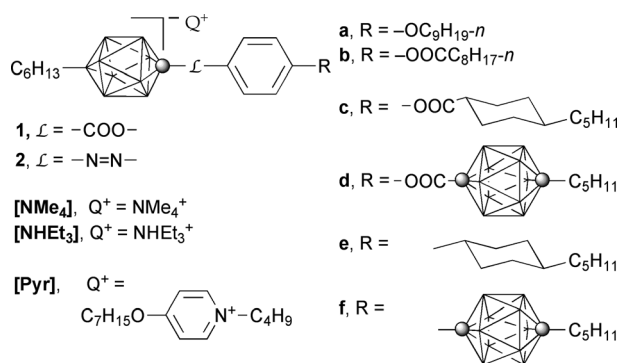
[*a*]Organic Materials Research Group, Department of Chemistry, Vanderbilt University, Nashville, TN, 37235, USA
[*b*]Nanotechnology Research Institute, National Institute of Advanced Industrial Science and Technology, AIST Kansai Centre, Midorigaoka 1-8-31, Ikeda, Osaka, 536-8577, Japan

**Fig. 1** The structures of the [*closo*-1-CB₉H₁₀]⁻ and [*closo*-1-CB₁₁H₁₂]⁻ clusters (**A** and **B**), and ion pairs of their 1,10- (**IA**) and 1,12-disubstituted (**IB**) derivatives with the counterion Q⁺. Q represents a metal or an onium fragment such as ammonium or pyridinium. Each vertex represents a BH fragment and the spheres are carbon atoms.

**Fig. 2** Structures of series **1** and **2**. Each vertex represents a BH fragment and the spheres are carbon atoms.

interactions with π substituents and consequently better control of photophysical properties of 10-vertex cluster derivatives (including those of **A**) than their 12-vertex counterparts, such as derivatives of **B**.[36,38,40]

The unusual properties of *closo*-boranes prompted us to explore clusters **A** and **B** as structural elements of ILCs and to develop a new class of conductive mesogenic metal salts. As the first step towards this goal, we focused on two series of disubstituted derivatives of [*closo*-1-CB$_9$H$_{10}$]$^-$ (**IA**), which can be accessed from the recently reported[41] isomerically pure [*closo*-1-CB$_9$H$_8$-1-COOH-10-I]$^-$. Here, we report the preparation of the first calamitic ILCs based on the [*closo*-1-CB$_9$H$_{10}$]$^-$ cluster (**A**) and investigation of two series of compounds, esters **1** and diazenes **2**, with three different cations Q$^+$ (Fig. 2). We establish fundamental structure–property relationships for these ILCs using polarizing optical microscopy (POM), differential scanning calorimetry (DSC), and powder X-ray diffraction (XRD). We also briefly investigate the photophysical behavior of two mesogens in solution and in the neat state.
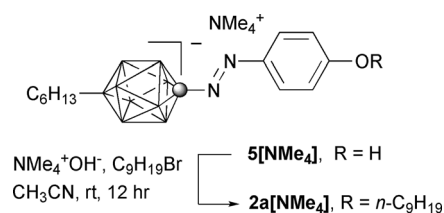
## Results and discussion

### Synthesis

Esters **1a[NMe$_4$]**–**1f[NMe$_4$]** were prepared from carboxylic acid **3[NMe$_4$]** and phenols **4a**–**4f** using dicyclohexylcarbodiimide (DCC) and catalytic amounts of 4-dimethylaminopyridine (DMAP) in CH$_2$Cl$_2$ following a general literature procedure[42] (Scheme 1). The preparation of phenols **4a**,[34] **4b**,[43] **4c**,[35] **4d**,[35] and **4f**[33] has been reported before.
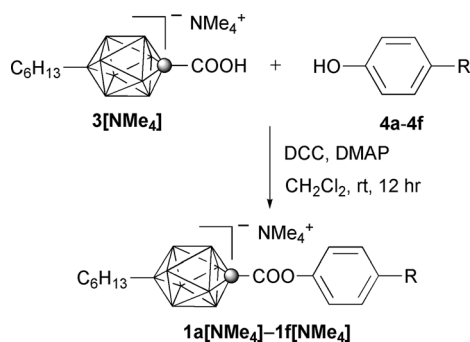


**Scheme 1** Synthesis of esters **1[NMe$_4$]**

Diazene **2a[NMe$_4$]** was prepared by alkylation of azophenol **5[NMe$_4$]** with 1-bromononane following a similar procedure that was described for the methylation of the parent azophenol[44] (Scheme 2).

Diazenes **2b**–**2d** were prepared by esterification of azophenol **5[NMe$_4$]** with acid chlorides **6b**–**6d** in CH$_2$Cl$_2$ in the presence of Et$_3$N (Scheme 3). Complete exchange of counterion NMe$_4^+$ for NHEt$_3^+$ was observed for diazenes **2b** and **2d** after isolation of the crude product by column chromatography. Acid chlorides **6c**[45] and **6d**[39] were prepared using literature protocols.

Esters **1a[Pyr]**–**1f[Pyr]** and diazenes **2a[Pyr]**–**2d[Pyr]** were prepared by exchange of the NMe$_4^+$ or NHEt$_3^+$ cation for *N*-butyl-4-heptyloxypyridinium using bromide **7** in a biphasic CH$_2$Cl$_2$/H$_2$O system.

Both carboxylic acid **3[NMe$_4$]** and azophenol **5[NMe$_4$]** were prepared from iodides **8[NMe$_4$]**[41] and **9[NMe$_4$]**, respectively, using Negishi coupling[46,47] with 12-fold excess hexylzinc chloride (Scheme 4). The electron-rich tricyclohexylphosphine ligand, PCy$_3$, was conveniently generated *in situ* from air-stable [HPCy$_3$]BF$_4$. The choice of the ligand was dictated by its



**Scheme 2** Preparation of diazene **2a[NMe$_4$]**
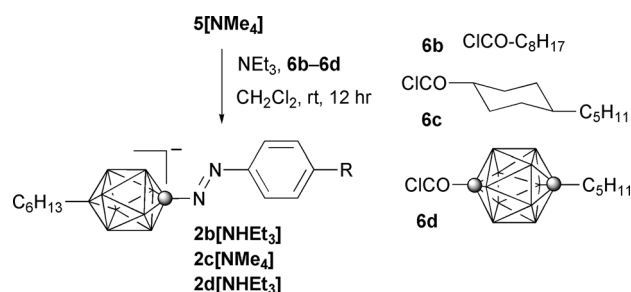


**Scheme 3** Synthesis of diazenes **2**.
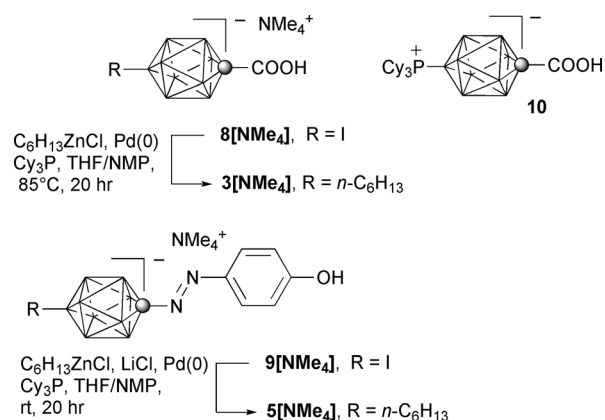


**Scheme 4** Preparation of intermediates **3[NMe$_4$]** and **5[NMe$_4$]**.
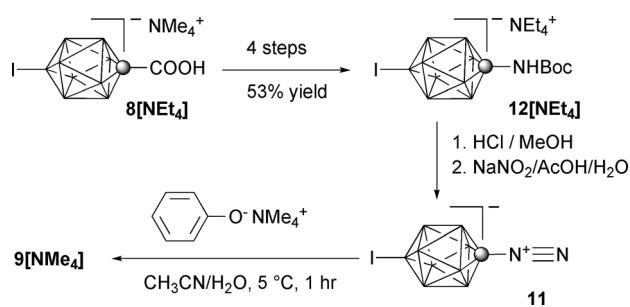
**Scheme 5** Preparation of dinitrogen derivatives **11**.

reported efficiency in catalysis of coupling reactions of alkylzinc reagents with a broad range of unactivated iodides, bromides and chlorides, and excellent functional group tolerance.[48] The carboxyl group of acid **8[NMe₄]** tolerated coupling reaction conditions at elevated temperatures, whereas what appeared to be reduction of the azo group, as well as loss of symmetry, in the {*closo*-1-CB₉} cluster was observed in azophenol **9[NMe₄]** under similar conditions. The addition of LiCl permitted the coupling reaction of **9[NMe₄]** to occur at room temperature, presumably due to increased reactivity and solubility of the organozinc reagent.[49] In reactions of **8[NMe₄]** with fewer equivalents of the organozinc reagent, the formation of phosphonium zwitterion **10** by-product was observed. For instance, with 5 equivalents of hexylzinc chloride the phosphonium by-product was isolated in about 3% yield and partially characterized.

Azophenol **9[NMe₄]** was prepared by azo-coupling of [*closo*-1-CB₉H₈-1-N₂-10-I] (**11**) and tetramethylammonium phenolate (Scheme 5). Dinitrogen species **11**[50] was prepared in 88% yield starting from carbamate **12[NEt₄]** using a procedure developed for the preparation of the parent dinitrogen derivative [*closo*-1-CB₉H₉-1-N₂].[44] The carbamate was prepared in a four-step modified Curtius rearrangement starting from the iodo acid **8[NEt₄]** in a procedure analogous to that described for the protected parent amine [*closo*-1-CB₉H₉-1-NHBoc][NEt₄].[44] This method represents a marked improvement over our previous

synthesis of the iodo amine [*closo*-1-CB₉H₈-1-NH₃-10-I].[41] Iodination of the amine [*closo*-1-CB₉H₉-1-NH₂]⁻ with *N*-iodo-succinimide in MeCN at ambient temperature, gave the 6-iodo isomer as the only detected product instead of the expected [*closo*-1-CB₉H₈-1-NH₂-10-I].

## Liquid crystalline properties

Transition temperatures and associated enthalpies for compounds **1[Pyr]** and **2[Pyr]** are shown in Tables 1 and 2. Phase structures were partially assigned by comparison of POM results with published textures for reference compounds,[51] established trends in thermodynamic stability,[52] and on the basis of powder XRD results for three mesogens. The tetramethylammonium salts (**1a[NMe₄]**–**1b[NMe₄]**, **2a[NMe₄]** and **2c[NMe₄]**) and the two triethylammonium salts (**2b[NHEt₃]** and **2d[NHEt₃]**) are non-mesogenic solids with melting points higher than those of the pyridinium salts.
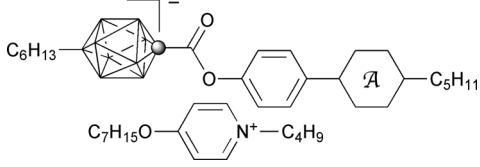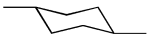
All three-ring pyridinium salts and two-ring diazene **2a[Pyr]** exhibit enantiotropic SmA phases. In addition, most esters display enantiotropic crystalline and soft crystalline polymorphism. Esters **1a[Pyr]**, **1b[Pyr]** and diazene **2b[Pyr]** do not form liquid crystalline phases even on cooling. For instance, the isotropic phase of diazene **2b[Pyr]** could be supercooled by 15 K before crystallization.

The most interesting polymorphism is displayed by esters **1e[Pyr]** and **1f[Pyr]** for which DSC analysis revealed two phases below the SmA phase. The enthalpy of the transition from the SmA is less than a half of the isotropization enthalpy in both esters, and the two lower phases are separated by a first-order transition of 3.2 kJ mol⁻¹ for **1e[Pyr]** (Fig. 3) and 1.5 kJ mol⁻¹ for **1f[Pyr]**. Optical observations of **1f[Pyr]** revealed pseudo-isotropic regions present in both soft crystalline phases, which is indicative of a non-tilted phase (Fig. 4). Both phases exhibit "broken fan" textures characteristic for a crystalline E phase, with the lower temperature phase having sharper features and higher viscosity. This assignment, however, is inconsistent with the absence of weakly birefringent regions expected to form in

**Table 1** Transition temperatures (°C) and enthalpies (kJ mol⁻¹, in parentheses) for selected compounds



| R | $L = -COO-$ (**1[Pyr]**) | $L = -N{=}N-$ (**2[Pyr]**) |
|---|---|---|
| **a** —O—C₈H₁₇ | Cr₁•53•Cr₂•127•Cr₃•151•I (15.4) (4.5) (20.6) | Cr•93•SmA•115•I (21.9) (9.6) |
| **b** | Cr₁•64•Cr₂•101•X•107•I (9.2) (3.4) (15.1) | Cr•96•I (40.9) |
| **c** | Cr•102•SmA•164•I (43.7) (7.0) | Cr₁•70•Cr₂•106•SmA•139•I (8.8) (21.1) (6.0) |
| **d** | Cr₁•94•X•162•SmA•180•I (22.7) (11.0) (9.4) | Cr•136•SmA•151•I (46.9) (7.4) |

**Table 2** Transition temperatures (°C) and enthalpies (kJ mol$^{-1}$, in parentheses) for esters **1e[Pyr]** and **1f[Pyr]**

| | | |
|---|---|---|
| **1e[Pyr]** A = | *(cyclohexyl ring structure)* | Cr•128•(X'•129)•X•153•SmA•163•I (19.3) (3.2) (2.4) (4.5) |
| **1f[Pyr]** A = | *(carborane cage structure)* | Cr•120•X'•145•X•166•SmA•187•I (18.1) (1.5) (4.2) (11.4) |
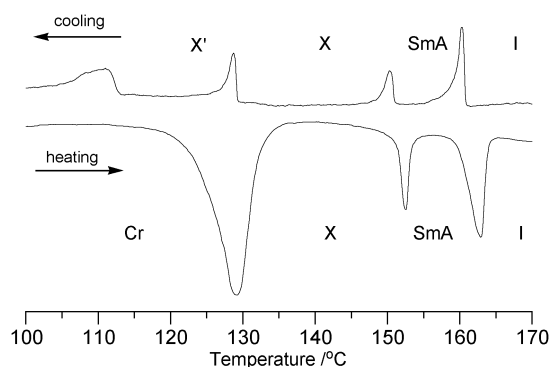
**Fig. 3** DSC trace of ester **1e[Pyr]**; heating rate = 5 K min$^{-1}$.
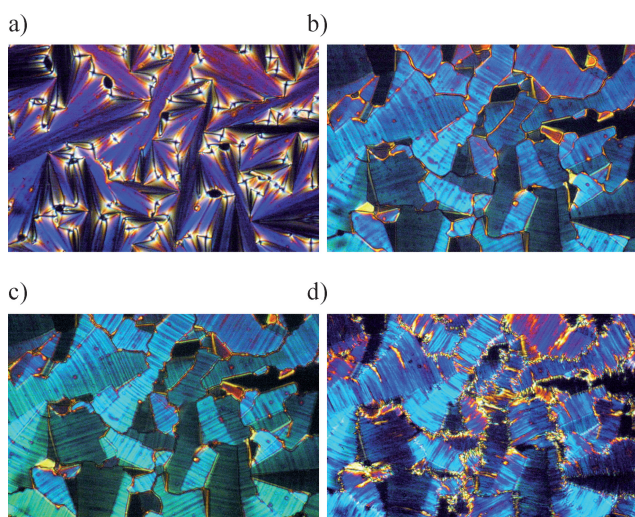
**Fig. 4** Optical textures of **1f[Pyr]** obtained for the same region of the sample upon cooling at (a) 173 °C (SmA), (b) 150 °C (X), (c) 125 °C (X') and (d) 90 °C (Cr). Magnification ×50.

place of homeotropic domains of SmA. After applying mechanical stress, the higher temperature soft crystalline phase quickly restores the original texture, while the lower temperature phase is more viscous and the change is permanent. Further cooling of the sample leads to crystallization and change of the texture (Fig. 4(d)).

Among other esters, **1d[Pyr]** exhibits noteworthy polymorphism. Its DSC appears similar to that of **1f[Pyr]** (Fig. 3) with a broad high-energy transition at 97 °C followed by two transitions, X–SmA and SmA–I. The last two transitions have comparable energies (Table 1) and undergo little supercooling, while the transition at 97 °C is significantly supercooled. The texture of the unidentified phase X below the SmA phase is similar to that of an E phase (Fig. 5) and significantly different from that of a crystalline phase below the X phase. Despite similarity of the textures, the X phase observed for **1d[Pyr]** and X and X' phases found in **1e[Pyr]** and **1f[Pyr]** may have different structures.

In general, the mesophase stability in both series increases with the increasing size of the substituent R and is the highest for the carborane derivatives **1f[Pyr]** and **1d[Pyr]**. A comparison of the two series demonstrates that esters **1[Pyr]** generally have higher clearing temperatures and richer polymorphism than the diazenes **2[Pyr]**. Among the two-ring mesogens, only diazene **2a[Pyr]** exhibits a SmA phase. A replacement of the CH$_2$ group in **2a[Pyr]** with C=O in **2b[Pyr]** results in elimination of mesogenic behavior. This is consistent with the generally observed
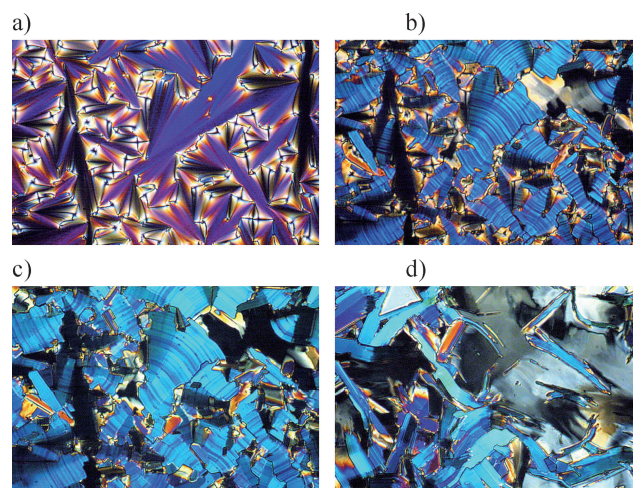
**Fig. 5** Optical textures of **1d[Pyr]** obtained for the same region of the sample upon cooling at (a) 170 °C (SmA), (b) 161 °C (phase X growing from SmA), (c) 150 °C (X) and (d) 80 °C (Cr). Magnification ×50.

higher mesophase stability for alkoxyazobenzenes than for their alkanoyloxy analogues.[53]

*N*-Butyl-4-hepyloxypyridinium bromide (**7**) is not mesogenic and melts at 34 °C to an isotropic liquid. Some 4-substituted pyridinium salts were reported to be mesogenic, but they require long alkyl chains.[21]

### Powder X-ray diffraction (XRD)

Two close structural analogous, ester **1d[Pyr]** and diazene **2d[Pyr]**, and also ester **1f[Pyr]** were investigated by powder X-ray diffraction to determine their phase structures. Data were collected at several temperatures on cooling from the isotropic phase, and XRD results are shown in Fig. 6 and also tabulated in ESI.†

The XRD results confirmed the SmA phase as the high-temperature phase in all three compounds. The diffractograms consist of a single sharp reflection in the small-angle region (001) followed by up to three higher-order reflections (00*l*) with the reciprocal ratio of *d*-spacing 1 : 2 : 3 : 4 (Fig. 6). The wide-angle region of the high-temperature phase diffractograms shows a broad halo in which two maxima can be distinguished at about $d = 5.5$ Å and $d = 4.5$ Å in two compounds (**1d[Pyr]** and **2d[Pyr]**,



Fig. 6(b)) and only one broad maximum at $d \approx 5.3$ Å in ester **1f[Pyr]** (Fig. 6(a)). The maximum with the lower *d* value can be attributed to the average alkyl chain–alkyl chain correlation distance, while the maxima with $d > 5$ Å can be attributed to the correlation involving larger structural units such as the boron clusters in the segregated ionic layer. Similar double haloes have been observed for siloxanes ($d = 7.0$ and 4.6 Å),[54,55] and fluoroalkyl-containing mesogens ($d = 5.2$ and 4.6 Å)[56] in which the large groups microsegregate.

The phases observed below the SmA phase in esters **1d[Pyr]** and **1f[Pyr]** and diazene **2d[Pyr]** have preserved the lamellar structure, as evident from sharp and more intense higher-order (00*l*) reflections. Their diffractograms also exhibit a number of additional wide-angle reflections indicating increased order within the layers. The pattern observed for the soft crystalline phase of **1f[Pyr]** is consistent neither with an E nor a B phase. The gliding symmetry, associated with the herring-bone molecular order in the E phase, precludes the observed (100) and (010) reflections, and permits the (210) reflection, which is absent in the diffractogram. On the other hand, assumption of a hexagonal B phase (unit cell dimensions: $a = 10.4$ Å and $c = 25.5$ Å) leads to a *Z* value (molecules per lattice) of 1.9 (assuming a density of 1.0 g cm$^{-1}$), while the symmetry of the phase requires $Z = 1$. Instead, the observed pattern for the upper soft crystalline phase of **1f[Pyr]** could be assigned to an orthogonal phase with the unit cell dimensions: $a = 9.0$ Å, $b = 5.2$ Å, $c = 25.7$ Å and $Z = 0.92$ (Fig. 6(a)). A possible structure of this phase may involve alternating ionic and hydrophobic layers with the period of 25.7 Å, and a two-dimensional rectangular lattice with the unit cell containing two molecules, the anion and the cation.

The lower temperature soft crystalline phase exhibits additional reflections, which are indicative of a more organized phase, presumably crystallization of the microsegregated ionic region of the sample. A similar pattern was observed for phase X in ester **1d[Pyr]** (Fig. 6(b)) in which the number of reflections is higher than might be expected for a B-like phase, but significantly lower than that observed for a crystalline phase of diazene **2d[Pyr]** grown from the SmA phase.[57] Unambiguous identification of these phases and understanding of their structures will require more detailed studies of oriented samples and single-crystal analysis.

A comparison of the layer spacing *c* with the molecular length *L* calculated for a model of the fully extended mesogen indicates that the molecules are organized in monolayers with significant interdigitation of the alkyl chains ($c < L$) in all three compounds. The calculated degree of the interdigitation, $I = (L - c)/L$, in the SmA phase was higher for **1d[Pyr]** and **2d[Pyr]** (0.18) than for ester **1f[Pyr]** (0.14). This value decreases in the X phase of **1d[Pyr]**, increases in the crystal phase of **2d[Pyr]**, and stays practically unchanged in the soft crystalline phases of **1f[Pyr]** relative to that in the SmA phase (Table 3). Incidentally, the layer spacing *d* is about double of the distance between the nitrogen atom and the tip of the heptyloxy chain in the pyridinium ion.

### Photophysical properties

Electronic absorption spectra demonstrated that ester **1e[Pyr]** is transparent above 280 nm (Fig. 7a). The single absorption peak
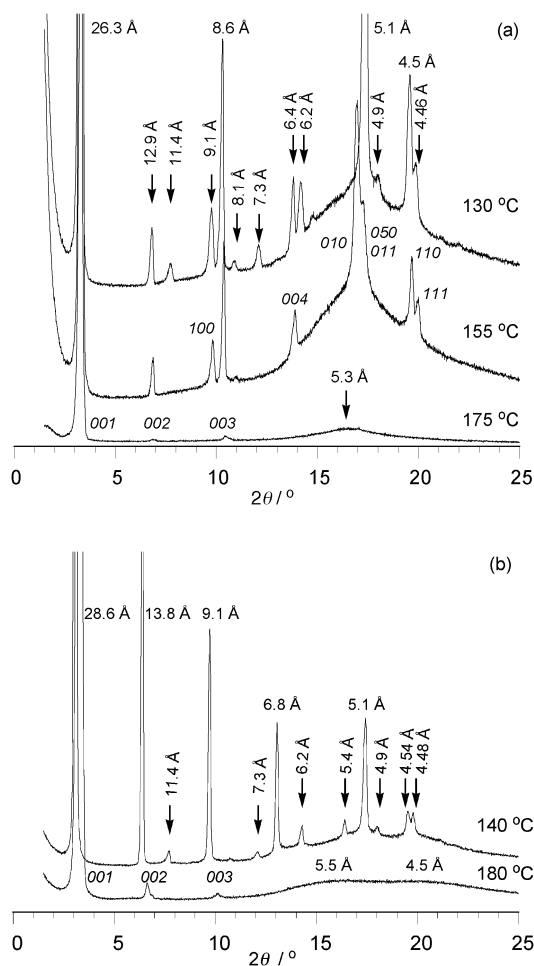
Fig. 6   Stacked X-ray diffraction patterns for (a) **1f[Pyr]** obtained at 175 °C (SmA, $c = 25.8$ Å), 155 °C (X, $a = 9.0$ Å, $b = 5.2$ Å, $c = 25.7$ Å) and 130 °C (X′), and (b) **1d[Pyr]** at 180 °C (SmA, $c = 26.6$ Å) and 140 °C (X).

This journal is © The Royal Society of Chemistry 2009

*J. Mater. Chem.*, 2009, **19**, 4805–4812 | 4809

**Table 3** The molecular interdigitation in selected phases

| Compound | Length $L^a$/Å | $T$/°C | Phase | Interdigitation[b] $I = (L - c)/L$ |
|---|---|---|---|---|
| **1d[Pyr]** | 32.3 | 180 | SmA | 0.18 |
| | | 140 | X | 0.15 |
| **2d[Pyr]** | 31.7 | 140 | SmA | 0.18 |
| | | 100 | Cr | 0.21 |
| **1f[Pyr]** | 29.8 | 175 | SmA | 0.14 |
| | | 155 | X | 0.14 |
| | | 130 | X' | 0.13 |

[a] Most extended molecular conformation optimized at the HF/6-31G(d) level of theory. See ESI.† [b] The cell constant $c$ is calculated from $d_{002}$.
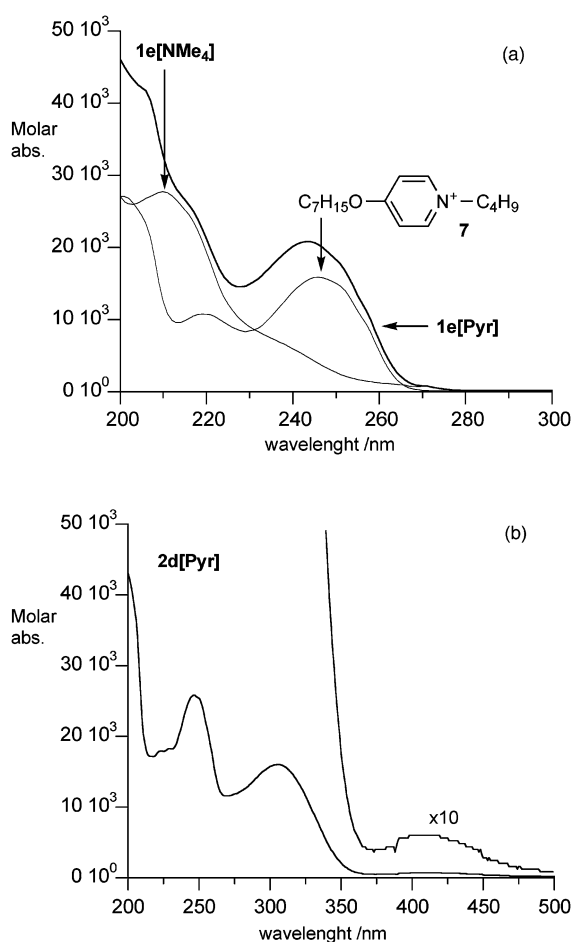




**Fig. 7** Electronic absorption spectra of (a) ester **1e[NMe₄]** (thin line), pyridinium bromide **7** (thin line), and **1e[Pyr]** (thick line), and (b) diazene **2d[Pyr]** recorded in MeCN.

at 243 nm (log $\varepsilon$ = 4.32) and a large absorbance at 200 nm (log $\varepsilon$ = 4.65) observed for **1e[Pyr]** in MeCN results from an overlap of high-energy absorbance of the anion **1e** (210 nm tailing to 280 nm, log $\varepsilon$ = 4.44) and pyridinium chromophores (246 nm, log $\varepsilon$ = 4.20). Practically identical results were obtained for **1e[Pyr]** in 1,2-dichloroethane (248 nm, log $\varepsilon$ = 4.30). No evidence of intermolecular charge-transfer between the {*closo*-1-CB₉} cluster and the pyridinium was found.

The diazene **2d[Pyr]** exhibits three distinct absorption maxima (Fig. 7(b)). The high energy maximum at 247 nm (log $\varepsilon$ = 4.41) is related to the pyridinium chromophore, while the two lower energy maxima at 305 nm (log $\varepsilon$ = 4.20) and 410 nm (log $\varepsilon$ = 2.7) are attributed to the phenylazo group. The latter two, identified as $\pi \rightarrow \pi^*$ and n $\rightarrow \pi^*$ transitions, respectively, are similar to those observed for the parent [*closo*-1-CB₉H₉-1-(N=N–C₆H₄OMe-4)]⁻ anion for which the analogous transitions were found at 319 nm (log $\varepsilon$ = 4.23) and 407 nm (log $\varepsilon$ = 2.8).[44]

An attempt to induce charge separation and transfer in ester **1d[Pyr]** and in diazene **2d[Pyr]** were unsuccessful. Irradiation of the TiO₂ charge generation layer deposited on the ITO conductive layer of an electro-optical cell containing the ester or direct irradiation of the diazene sample in the electrooptical cell with 337 nm laser beam did not result in photocurrent generation.

## Summary and conclusions

Results show that the [*closo*-1-CB₉H₁₀]⁻ anion (**A**) is an effective and unusual structural element of ionic liquid crystals in which the negative charge is fully delocalized and the anion is non-nucleophilic. This implies no specific interactions between the ions. The study of two series of mesogens, **1** and **2**, demonstrate that all three-ring and even some two-ring (**2a[Pyr]**) compounds exhibit a partially interdigitated monolayer SmA phase when the pyridinium counterion is present. In addition, esters **1[Pyr]** exhibit a rich soft crystalline and crystalline polymorphism, which resembles behavior of typical non-ionic calamitic mesogens. Unlike in conventional calamitics, soft crystalline phases of esters **1[Pyr]** appear to adopt two mutually perpendicular layered molecular organization. Esters **1** are transparent above 280 nm, while diazenes **2** are potentially photoresponsive mesogens.

The presented work opens a possibility for further manipulation with the structure and fine-tuning of mesogenic and photophysical properties. Of particular interest are anions, which may lead to ambient temperature mesophases of their metal salts with a broad electrochemical window. Such materials are desired for devices in which cation transport is important.

## Experimental

Optical microscopy was performed using a PZO Biolar microscope equipped with an HCS402 Instec hot stage. Thermal analysis was obtained using a TA Instruments 2920 DSC. Transition temperatures (onset) and enthalpies were obtained using small samples (~0.5 mg) and a typical heating/cooling rate of 5 K min⁻¹ under a flow of nitrogen gas. UV spectra were recorded in MeCN and molar absorption was obtained from a Beer's law plot of 4–5 concentrations. XRD measurements were carried out on unoriented and uncovered samples placed on a temperature-controlled glass plate using Rigaku RINT2000 X-ray diffractometer (Cu-Kα₁ = 1.5405 Å) and a custom-made heater. XRD patterns were collected in the range of 1.5°–35° on cooling. Layer spacings (cell constant $c$) were determined form the (002) reflection.

Photocurrent generation was investigated in 17 μm thick electro-optical cells using methods and setups described before.[58] The cell used for studies of ester **1d[Pyr]** had an TiO₂ layer deposited on the top of the conductive ITO layer.[19] Detailed procedures and analytical data for all compounds are provided in ESI.†

## General procedure for preparation of 1[Pyr] and 2[Pyr]

$N$-Butyl-4-heptyloxypyridinium bromide (**7**, 1.0 equivalent) was added to a solution of ester **1[NMe₄]** or diazene **2[NMe₄]** or **2[NHEt₃]** in $CH_2Cl_2$ and a white precipitate formed. Water was added, and the biphasic system was stirred vigorously until all the precipitate had dissolved. The $CH_2Cl_2$ layer was separated, and the aqueous layer was extracted with additional $CH_2Cl_2$. The $CH_2Cl_2$ layers were combined, dried ($Na_2SO_4$), and evaporated giving a white (**1[Pyr]**) or yellow (**2[Pyr]**) crystalline solid, which was recrystallized from aqueous alcohol. The crystals were dried under vacuum for several hours.

## General procedure for preparation of esters 1a[NMe₄]–1f[NMe₄]

Phenol **4** (1.5 equivalents) was added to a colorless solution of [*closo*-1-CB₉H₈-1-COOH-10-C₆H₁₃]⁻NMe₄⁺ (**3[NMe₄]**), DCC (1.0 equivalent), and DMAP (0.1 equivalents) in anhydrous $CH_2Cl_2$. The mixture was stirred overnight at rt, and the reaction progress was monitored by TLC ($R_f = 0.5$, $CH_3CN–CH_2Cl_2$, 1 : 9). The solvent was removed *in vacuo*, and the crude product was isolated by column chromatography (SiO₂, $CH_3CN–CH_2Cl_2$, 1 : 9). The resulting ester was washed with hot hexane and recrystallized from EtOH–$H_2O$ or MeOH–$H_2O$. Esters **1a[NMe₄]** and **1b[NMe₄]** were difficult to crystallize and were converted directly to $N$-butyl-4-heptyloxypyridinium salts (**1[Pyr]**).

## Preparation of [*closo*-1-CB₉H₈-1-(N=N–C₆H₄-OC₉H₁₉-4)-10-C₆H₁₃]⁻NMe₄⁺ (2a[NMe₄])

A solution of 1-bromononane (0.08 mL, 0.4 mmol) in anhydrous $CH_3CN$ (2 mL) was added to an orange solution of azophenol **5[NMe₄]** (0.042 g, 0.106 mmol, about 60% pure; contaminated with NMP) and NMe₄⁺OH⁻·5H₂O (0.06 g, 0.32 mmol) in anhydrous $CH_3CN$ (2 mL). The solution was stirred at 50 °C for 4 h. The reaction mixture was worked up and the product was isolated as described for esters **1[NMe₄]** and used for the preparation of **2a[Pyr]** without crystallization.

## General procedure for preparation of diazenes 2b[NHEt₃], 2c[NMe₄] and 2d[NHEt₃]

A solution of acid chloride **6** (4.0 equivalents) in anhydrous $CH_2Cl_2$ was added to an orange solution of azophenol **5[NMe₄]** (about 60% pure; contaminated with NMP) and NEt₃ (5.0 equivalents) in anhydrous $CH_2Cl_2$. The bright yellow solution was stirred for 12 h, and reaction progress was monitored by TLC ($R_f = 0.5$ in $CH_3CN–CH_2Cl_2$, 1 : 9). The reaction mixture was worked up and the product was isolated as described for esters **1[NMe₄]**. Without crystallization, the resulting diazenes **2b[NHEt₃]**, **2c[NMe₄]** or **2d[NHEt₃]** were converted to the pyridinium salts **2[Pyr]**.

## Acknowledgements

## References

1 K. Binnemans, *Chem. Rev.*, 2005, **105**, 4148–4204, and references therein.
2 M. Yoshio, T. Mukai, K. Kanie, M. Yoshizawa, H. Ohno and T. Kato, *Adv. Mater.*, 2002, **14**, 351–354; T. Kato, *J. Am. Chem. Soc.*, 2006, **128**, 5570–5577; M. Yoshio, T. Mukai, H. Ohno and T. Kato, *J. Am. Chem. Soc.*, 2004, **126**, 994–995.
3 T. Ichikawa, M. Yoshio, A. Hamasaki, T. Mukai, H. Ohno and T. Kato, *J. Am. Chem. Soc.*, 2007, **129**, 10662–10663.
4 S. Yazaki, Y. Kamikawa, M. Yoshio, A. Hamasaki, T. Mukai, H. Ohno and T. Kato, *Chem. Lett.*, 2008, **37**, 538–539.
5 Y. Grabovskiy, A. Kovalchuk, A. Grydyakina, S. Bugaychuk, T. Mirnaya and G. Klimusheva, *Liq. Cryst.*, 2007, **34**, 599–603.
6 H. Shimura, M. Yoshio, K. Hoshino, T. Mukai, H. Ohno and T. Kato, *J. Am. Chem. Soc.*, 2008, **130**, 1759–1765.
7 Y. Abu-Lebdeh, A. Abouimrane, P.-J. Alarco and M. Armand, *J. Power Sources*, 2006, **154**, 255–261.
8 N. Yamanaka, R. Kawano, W. Kubo, T. Kitamura, Y. Wada, M. Watanabe and S. Yanagida, *Chem. Commun.*, 2005, 740–742; R. Kawano, M. K. Nazeeruddin, A. Sato, M. Gratzel and M. Watanabe, *Electrochem. Commun.*, 2007, **9**, 1134–1138.
9 H. Ohno, *Bull. Chem. Soc. Jpn.*, 2006, **79**, 1665–1680; H. Ohno. *Electrochemical Aspects of Ionic Liquids*, Wiley, Honboken, NJ, 2005.
10 P. K. S. Antharjanam, V. A. Mallia and S. Das, *Liq. Cryst.*, 2004, **31**, 713–717.
11 K. Tanabe, T. Yasuda and T. Kato, *Chem. Lett.*, 2008, **37**, 1208–1209; K. Goossens, P. Nockemann, K. Driesen, B. Godoris, C. Gorller-Walrand, K. Van Hecke, L. Van Meervelt, E. Pouzet, K. Binnemans and T. Cardinaels, *Chem. Mater.*, 2008, **20**, 157–168; J. Yang, Q. Zhang, Z. Laiyang, S. Zhang, J. Li, X. Zhang and Y. Deng, *Chem. Mater.*, 2007, **19**, 2544–2550.
12 Z.-Q. Zhu, S. Xiang, Q.-Y. Chen, C. Chen, Z. Zeng, Y.-P. Cui and J. C. Xiao, *Chem. Commun.*, 2008, 5016–5018.
13 D. Ster, U. Baumeister, J. Chao Lorenzo, C. Tschierske and G. Israel, *J. Mater. Chem.*, 2007, **17**, 3393–3400.
14 F. Lo Celso, I. Pibiri, A. Triolo, R. Triolo, A. Pace, S. Buscemi and N. Vivona, *J. Mater. Chem.*, 2007, **17**, 1201–1208.
15 D. Haristoy and D. Tsiourvas, *Liq. Cryst.*, 2004, **31**, 697–703.
16 B. O'Regan and M. Gratzel, *Nature*, 1991, **353**, 737–740.
17 V. Busico, P. Corradini and M. Vacatello, *J. Phys. Chem.*, 1982, **86**, 1033–1034; V. Busico, P. Cernicchiaro, P. Corradini and M. Vacatello, *J. Phys. Chem.*, 1983, **87**, 1631–1635; J. D. Gault, H. A. Gallardo and H. Muller, *Mol. Cryst. Liq. Cryst.*, 1985, **130**, 163–177; K. Iwamoto, Y. Ohnuki, K. Sawada and M. Seno, *Mol. Cryst. Liq. Cryst.*, 1981, **73**, 95–103; C. M. Paleos, M. Arkas and A. Skoulios, *Mol. Cryst. Liq. Cryst.*, 1998, **309**, 237–250.
18 C. M. Gordon, J. D. Holbrey, A. R. Kennedy and K. R. Seddon, *J. Mater. Chem.*, 1998, **8**, 2627–2636; J. D. Holbrey and K. R. Seddon, *J. Chem. Soc., Dalton Trans.*, 1999, 2133–2139; P. H. J. Kouwer and T. M. Swager, *J. Am. Chem. Soc.*, 2007, **129**, 14042–14052.
19 J.-M. Suisse, L. Douce, S. Bellemin-Laponnaz, A. Maisse-François, R. Welter, Y. Miyake and Y. Shimizu, *Eur. J. Inorg. Chem.*, 2007, 3899–3905.
20 M. Tabrizian, A. Soldera, M. Couturier and C. G. Bazuin, *Liq. Cryst.*, 1995, **18**, 475–482; C. Cruz, B. Heinrich, A. C. Ribeiro, D. W. Bruce and D. Guillon, *Liq. Cryst.*, 2000, **27**, 1625–1631; L. Cui, V. Sapagovas and G. Lattermann, *Liq. Cryst.*, 2002, **29**, 1121–1132.
21 E. J. R. Sudholter, J. B. F. N. Engberts and W. de Jeu, *J. Phys. Chem*, 1982, **86**, 1908–1913; J. J. H. Nusselder, J. B. F. N. Engberts and H. A. Van Doren, *Liq. Cryst.*, 1993, **13**, 213–225.
22 D. Vorlander, *Ber. Dtsch. Chem. Ges.*, 1910, **43**, 3120–3135; R. Van Duen, J. Ramaekers, P. Nockemann, K. Van Hecke, L. Van Meervelt and K. Binnemans, *Eur. J. Inorg. Chem.*, 2005, **3**, 563–571; P. A. Winsor, in *Liquid Crystals and Plastic Crystals*, ed. G. W. Gray and P. A. Winsor, Horwood, New York, 1974, vol. 1, pp 225–254.
23 C. M. Paleos, D. Kardassi, D. Tsiourvas and A. Skoulios, *Liq. Cryst.*, 1998, **25**, 267–275.
24 W. Gao, L. Dickinson, F. G. Morin and L. Reven, *Chem. Mater.*, 1997, **9**, 3113–3120.
25 T. Ohtake, M. Ogasawara, K. Ito-Akita, N. Nishina, S. Ujiie, H. Ohno and T. Kato, *Chem. Mater.*, 2000, **12**, 782–789;

K. Kishimoto, T. Suzawa, T. Yokota, T. Mukai, H. Ohno and T. Kato, *J. Am. Chem. Soc.*, 2005, **127**, 15618–15623.

26 P. Kaszynski and A. G. Douglass, *J. Organomet. Chem.*, 1999, **581**, 28–38.

27 S. Korbe, P. J. Schreiber and J. Michl, *Chem. Rev.*, 2006, **106**, 5208–5249; B. Stibr, *Chem. Rev.*, 1992, **92**, 225–250; P. v. R. Schleyer and K. Najafian, *Inorg. Chem.*, 1998, **37**, 3454–3470.

28 C. A. Reed, *Acc. Chem. Res.*, 1998, **31**, 133–139; S. H. Strauss, *Chem. Rev.*, 1993, **93**, 927–942; I. Krossing and I. Raabe, *Angew. Chem., Int. Ed.*, 2004, **43**, 2066–2090.

29 A. S. Larsen, J. D. Holbrey, F. S. Tham and C. A. Reed, *J. Am. Chem. Soc.*, 2000, **122**, 7264–7272; M. Nieuwnhuyzen, K. R. Seddon, F. Teixidor, A. V. Puga and C. Viñas, *Inorg. Chem.*, 2009, **48**, 889–901.

30 J. W. Johnson and J. F. Brody, *J. Electrochem. Soc.*, 1982, **129**, 2213–2219.

31 S. V. Ivanov, W. J. Casteel and W. H. Bailey, *US Pat. Appl.*, 2007, US 2007189946; G. P. Pez, S. V. Ivanov, G. Dantsin, W. J. Casteel and J. F. Lehmann, *Eur. Pat. Appl.*, 2007, EP 1763099.

32 A. Januszko, K. M. More, S. Pakhomov, P. Kaszynski, M. O'Neill and M. D. Wand, *J. Mater. Chem.*, 2004, **14**, 1544–1553; A. Januszko, K. L. Glab, P. Kaszynski, K. Patel, R. A. Lewis, G. H. Mehl and M. D. Wand, *J. Mater. Chem.*, 2006, **16**, 3183–3192; M. Jasinski, A. Jankowiak, A. Januszko, M. Bremer, D. Pauluth and P. Kaszynski, *Liq. Cryst.*, 2008, **35**, 343–350.

33 K. Ohta, A. Januszko, P. Kaszynski, T. Nagamine, G. Sasnouski and Y. Endo, *Liq. Cryst.*, 2004, **31**, 671–682.

34 P. Kaszynski, A. Januszko, K. Ohta, T. Nagamine, P. Potaczek, V. G. Young, Jr. and Y. Endo, *Liq. Cryst.*, 2008, **35**, 1169–1190.

35 A. Januszko and P. Kaszynski, *Liq. Cryst.*, 2008, **35**, 705–710.

36 P. Kaszynski, K. K. Kulikiewicz, A. Januszko, A. G. Douglass, R. W. Tilford, S. Pakhomov, M. K. Patel, V. G. Young, Jr. in preparation.

37 For other recent publications see: B. Ringstrand, J. Vroman, D. Jensen, A. Januszko, P. Kaszynski, J. Dziaduszek and W. Drzewinski, *Liq. Cryst.*, 2005, **32**, 1061–1070; A. Januszko, K. L. Glab and P. Kaszynski, *Liq. Cryst.*, 2008, **35**, 549–553; T. Nagamine, A. Januszko, K. Ohta, P. Kaszynski and Y. Endo, *Liq. Cryst.*, 2008, **35**, 865–884.

38 P. Kaszynski, S. Pakhomov, K. F. Tesh and V. G. Young, Jr., *Inorg. Chem.*, 2001, **40**, 6622–6631.

39 A. G. Douglass, K. Czuprynski, M. Mierzwa and P. Kaszynski, *J. Mater. Chem.*, 1998, **8**, 2391–2398.

40 P. Kaszynski, S. Pakhomov and V. G. Young, Jr., *Collect. Czech. Chem. Commun.*, 2002, **67**, 1061–1083; S. Pakhomov, P. Kaszynski and V. G. Young, Jr., *Inorg. Chem.*, 2000, **39**, 2243–2245; A. Balinski, A. Januszko, J. E. Harvey, E. Brady, P. Kaszynski, V. G. Young, Jr., in preparation; P. Kaszynski, in *Anisotropic Organic Materials*, ed. R. Glaser and P. Kaszynski, ACS Symposia, Washington D.C., 2001; Vol. 798, p 68–82.

41 B. Ringstrand, A. Balinski, A. Franken and P. Kaszynski, *Inorg. Chem.*, 2005, **44**, 9561–9566.

42 B. Neises and W. Steglich, *Angew. Chem., Int. Ed.*, 1978, **17**, 522–524.

43 M. E. Neubert, P. J. Wildman, M. J. Zawaski, C. A. Hanlon, T. L. Benyo and A. D. Vries, *Mol. Cryst. Liq. Cryst.*, 1987, **145**, 111–158.

44 B. Ringstrand, P. Kaszynski and A. Franken, submitted.

45 N. Carr, G. W. Gray and D. G. McDonnell, *Mol. Cryst. Liq. Cryst.*, 1983, **97**, 13–28.

46 E. Erdik, *Tetrahedron*, 1992, **48**, 9577–9648.

47 P. Knochel and R. D. Singer, *Chem. Rev.*, 1993, **93**, 2117–2188.

48 J. Zhou and G. C. Fu, *J. Am. Chem. Soc.*, 2003, **125**, 12527–12530.

49 A. Krasovskiy, V. Malakhov, A. Gavryushin and P. Knochel, *Angew. Chem., Int. Ed.*, 2006, **45**, 6040–6044.

50 The original synthesis and the solid-state structure of **11** by M. Carr, A. Franken, P. Kaszynski and J. D. Kennedy, will be reported elsewhere.

51 D. Demus; L. Richter. *Textures of Liquid Crystals*, 2nd edn, VEB, Leipzig, 1980; G. W. Gray and J. W. G. Goodby, *Smectic Liquid Crystals-Textures and Structures*, Leonard Hill, Philadelphia, 1984; I. Dierking. *Textures of Liquid Crystals*, Wiley-VCH, Weinheim, 2003.

52 M. E. Neubert, in *Liquid Crystals: Experimental Study of Physical Properties and Phase Transitions*, ed. S. Kumar, Cambridge University Press, New York, 2001, and references therein.

53 R. Steinsträsser and L. Pohl, *Z. Naturforsch., Teil B*, 1971, **26**, 577–580.

54 R. A. Reddy, U. Baumeister, C. Keith, H. Hahn, H. Lang and C. Tschierske, *Soft Matter*, 2007, **3**, 558–570.

55 C. Keith, R. A. Reddy, A. Hauser, U. Baumeister and C. Tschierske, *J. Am. Chem. Soc.*, 2006, **128**, 3051–3066.

56 M. Prehm, X. H. Cheng, S. Diele, M. K. Das and C. Tschierske, *J. Am. Chem. Soc.*, 2002, **124**, 12072–12073.

57 See ESI†.

58 M. J. Sienkowska, H. Monobe, P. Kaszynski and Y. Shimizu, *J. Mater. Chem.*, 2007, **17**, 1392–1398.